Structural Isomerism in Silver Thioether Macrocyclic Chemistry: the Synthesis, Redox Properties and Crystal Structures of $[Ag_n([15]aneS_5)_n][PF_6]_n$, $[Ag_2([15]aneS_5)_2][BPh_4]_2$ and $[Ag([15]aneS_5)][B(C_6F_5)_4]$ ([15]aneS$_5$ = 1,4,7,10,13-pentathiacyclopentadecane)†

Alexander J. Blake,[a] David Collison,[b] Robert O. Gould,[a] Gillian Reid[a] and Martin Schröder*,[a]

[a] *Department of Chemistry, The University of Edinburgh, West Mains Road, Edinburgh EH9 3JJ, UK*

[b] *Department of Chemistry, The University of Manchester, Oxford Road, Manchester M13 9PL, UK*

Reaction of $AgNO_3$ with 1 molar equivalent of [15]aneS$_5$ (1,4,7,10,13-pentathiacyclopentadecane) in refluxing MeOH–water gives a colourless solution. Addition of excess of counter ion [PF_6^-, BPh_4^- or $B(C_6F_5)_4^-$] affords the colourless complexes $[Ag_n([15]aneS_5)_n][PF_6]_n$, $[Ag_2([15]aneS_5)_2][BPh_4]_2$ and $[Ag([15]aneS_5)][B(C_6F_5)_4]$ respectively in high yield. Single-crystal X-ray structural studies on these systems have revealed different cation stereochemistries as the counter ion is altered. Thus, $[Ag_n([15]aneS_5)_n][PF_6]_n$ crystallises in the orthorhombic space group *Iba2* with a = 25.713(3), b = 25.749(3), c = 11.6989(19) Å and Z = 16. The two independent infinite chains of cations in the structure are antiparallel. The stereochemistry at Ag^I is severely distorted octahedral through an [S_4 + S_2] donor set, Ag(1) ··· S(1) 3.219(5), Ag(1)–S(4) 2.659(5), Ag(1)–S(7) 2.651(6), Ag(1) ··· S(10) 3.075(7), Ag(1)–S(13) 2.564(6) Å, with one thioether donor from an adjacent $[Ag([15]aneS_5)]^+$ fragment asymmetrically bridging two metal centres, Ag(1)–S(1B) 2.742(5) Å. A similar geometry is observed at the second Ag ion, Ag(2) ··· S(1′) 3.263(5), Ag(2)–S(4′) 2.605(5), Ag(2) ··· S(7′) 2.964(8), Ag(2)–S(10′) 2.713(7), Ag(2)–S(13′) 2.637(6), Ag(2)–S(1D) 2.714(5) Å. The complex $[Ag_2([15]aneS_5)_2][BPh_4]_2$ crystallises in the triclinic space group $P\bar{1}$ with a = 11.462(3), b = 11.895(3), c = 27.019(10) Å, α = 78.503(18), β = 84.729(13), γ = 67.118(18)°, and Z = 2. The structure of the $[Ag_2([15]aneS_5)_2]^{2+}$ cation shows an unusual binuclear stereochemistry with [4 + 1] thioether donation to one silver(I) centre, Ag(2)–S(7′) 2.558(4), Ag(2)–S(10′) 2.623(5), Ag(2)–S(13′) 2.716(5), Ag(2)–S(1) 2.486(3), Ag(2) ··· S(1′) 3.131(3) Å, and [3 + 1] thioether donation to the other, Ag(1)–S(7) 2.529(3), Ag(1)–S(10) 2.608(4), Ag(1)–S(1′) 2.537(3), Ag(1) ··· S(1) 2.907(3) Å. Thus, one S-donor [S(1) and S(1′)] of each macrocycle bridges asymmetrically between the two metal centres. The complex $[Ag([15]aneS_5)][B(C_6F_5)_4]$ crystallises in the triclinic space group $P\bar{1}$ with a = 12.476(5), b = 13.658(7), c =15.608(6) Å, α = 108.300(22), β = 108.467(17), γ = 100.518(21)° and Z = 2. The structure contains discrete mononuclear $[Ag([15]aneS_5)]^+$ cations and $[B(C_6F_5)_4]^-$ anions. The geometry at Ag^I is asymmetric with all five thioether donors of the macrocycle interacting with the metal centre: Ag–S(1) 2.4712(19), Ag ··· S(4) 2.7262(20), Ag–S(7) 2.6847(21), Ag–S(10) 2.5621(19), Ag ··· S(13) 2.8813(19) Å. In MeCN solution $[Ag([15]aneS_5)]^+$ shows a chemically reversible Ag^I–Ag^{II} redox couple at $E_{\frac{1}{2}}$ = 0.76 V and a quasi-reversible Ag^I–Ag^0 couple at −0.37 V *vs.* ferrocene–ferrocenium. The intensely coloured d^9 silver(II) oxidation product has been observed by X- and Q-band ESR spectroscopy and the oxidation of Ag^I to Ag^{II} monitored spectroelectrochemically.

In recent years several groups including our own have been engaged in studies on complexes involving thioether macrocyclic ligands.[1,2] Interest in these systems stems from the observation that whereas acyclic thioether complexes tend to be susceptible to hydrolysis and demetallation,[3] macrocyclic thioethers generally allow preparation of relatively stable complexes. The inherent stability of the metal–macrocyclic fragment has enabled the electrochemical properties of these systems to be probed. Thus, we have shown that discrete single-electron redox couples can become accessible, *e.g.* Fe^{II}–Fe^{III},[4] Ni^{I}–Ni^{II}–Ni^{III},[5] Rh^{I}–Rh^{II}–Rh^{III},[6,7] Ir^{II}–Ir^{III},[8] Pd^{I}–Pd^{II}–Pd^{III}–Pd^{IV},[6,9] and Pt^{II}–Pt^{III}–Pt^{IV}.[10] We have applied electrochemistry, ESR and *in situ* electronic spectroscopy to study the processes occuring and to characterise the highly reactive products generated. In certain cases we have also demonstrated that there is a correlation between the stereochemical and electrochemical properties observed. Thus, for example in $[Rh([9]aneS_3)_2]^{3+}$ ([9]aneS$_3$ = 1,4,7-trithiacyclononane), stabilisation of Rh^{III}, Rh^{II} and Rh^{I} is attributed to the conformational flexibility of the two facially bound [9]aneS$_3$ ligands, enabling these units to accommodate the stereochemical preferences of the different rhodium oxidation states.[6,7]

More recently we have shown that [9]aneS$_3$, [18]aneS$_6$, [18]aneN$_2$S$_4$, Me$_2$[18]aneN$_2$S$_4$ and [15]aneS$_2$O$_3$‡ can also form stable complexes with d^{10} silver(I)[11,12] and gold(I)[13] centres. Indeed, such co-ordination has led to the preparation and structural characterisation of a unique series of complexes,

† *Supplementary data available:* see Instructions for Authors, *J. Chem. Soc., Dalton Trans.*, 1993, Issue 1, pp. xxiii–xxviii.

Non-SI unit employed: G = 10^{-4} T.

‡ [18]aneS$_6$ = 1,4,7,10,13,16-Hexathiacyclooctadecane, [18]aneN$_2$S$_4$ = 1,4,10,13-tetrathia-7,16-diazacyclooctadecane, Me$_2$[18]aneN$_2$S$_4$ = 7,16-dimethyl-1,4,10,13-tetrathia-7,16-diazacyclooctadecane, [15]aneS$_2$O$_3$ = 1,4,7-trioxa-10,13-dithiacyclopentadecane

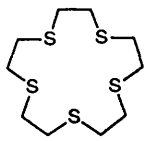

[15]aneS$_5$

$[Au([9]aneS_3)_2]^{+/2+/3+}$.[13] The complex $[Au([9]aneS_3)_2]^{2+}$ represents the first fully characterised example of mononuclear Au^{II}. Also, we have achieved stabilisation of silver(II) radical species *via* macrocyclic thioether co-ordination. For example, electrochemical studies on the octahedral complexes $[Ag([18]aneS_6)]^+$, $[Ag([9]aneS_3)_2]^+$ and $[Ag([18]aneN_2S_4)]^+$ show Ag^I–Ag^{II} couples at $E_{\frac{1}{2}} = +1.00$, $+0.75$ and $+0.65$V *vs.* ferrocene–ferrocenium, respectively.[11,12,14] The silver(I) precursors are structurally interesting since they each show the d^{10} ion bound to a distorted octahedral arrangement of the donor atoms. This suggests that the co-ordination geometry adopted is determined mainly by the 'donacity' and conformational requirements of the macrocyclic ligand. These observations prompted us to investigate the co-ordination of Ag^I with the pentathia crown [15]aneS$_5$ (1,4,7,10,13-pentathiacyclopentadecane) since this introduces a severe stereochemical mismatch between the predicted preferences of the silver(I) ion (octahedral or tetrahedral) and the macrocycle (five-co-ordinate). We were interested to determine whether such a combination would induce unusual structural and/or electrochemical features.

Chemical oxidation of $[Ag([18]aneS_6)]^+$, $[Ag([9]aneS_3)_2]^+$ and $[Ag([18]aneN_2S_4)]^+$ leads to formation of intensely coloured blue or purple paramagnetic complexes; these highly reactive species have so far eluded full characterisation, but ESR spectroscopic data are consistent with their assignment as mononuclear silver(II) species.[14,15] We now report the synthesis and single-crystal X-ray structures of the isomeric series $[Ag_n([15]aneS_5)_n][PF_6]_n$, $[Ag_2([15]aneS_5)_2][BPh_4]_2$ and $[Ag([15]aneS_5)][B(C_6F_5)_4]\cdot 2.5CH_2Cl_2$. A discussion of the redox properties of the PF_6^- salt is also presented, together with evidence from X- and Q-band ESR spectroscopy and *in situ* electronic spectroscopy for the formation of a paramagnetic silver(II) oxidation product. Several other silver(I) complexes incorporating saturated[15,16] and unsaturated[17] thioether macrocycles have been reported. A communication on this work has appeared previously.[18]

Results and Discussion

Reaction of $AgNO_3$ with 1 molar equivalent of [15]aneS$_5$ in refluxing MeOH–water for 30 min affords a colourless solution. Addition of an excess of NH_4PF_6, $NaBPh_4$ or $Li[B(C_6F_5)_4]$ (the perfluorinated derivative of $LiBPh_4$) and recrystallisation of the product from $MeNO_2$–diethyl ether gives a white, light-sensitive product. In each case FAB mass spectrometry reveals molecular ion peaks (M^+) at $m/z = 407$ and 409 corresponding to $[^{107}Ag([15]aneS_5)]^+$ and $[^{109}Ag([15]aneS_5)]^+$ respectively. This, together with IR spectroscopic and microanalytical data, confirms the empirical formulation $[Ag([15]aneS_5)]X$ [X = PF_6^-, BPh_4^- or $B(C_6F_5)_4^-$] for the products. In order to ascertain the stereochemistry of the cationic species and the conformation of the crown thioether in these systems, single-crystal X-ray determinations were undertaken.

Colourless crystals were obtained by slow evaporation from a solution of $[Ag([15]aneS_5)]BPh_4$ in $MeNO_2$. The structure determination shows (Fig. 1) a very unusual and unexpected dimeric $[Ag_2([15]aneS_5)_2]^{2+}$ cation, involving [3 + 1] S-donor co-ordination at one silver(I) centre, *via* two thioether donor atoms of one [15]aneS$_5$ macrocycle, Ag(1)–S(7) 2.529(3), Ag(1)-S(10) 2.608(4) Å, and one thioether donor atom from a second [15]aneS$_5$ crown, Ag(1)-S(1′) 2.537(3) Å. Atom S(1) is involved in a further long-range, weak interaction,

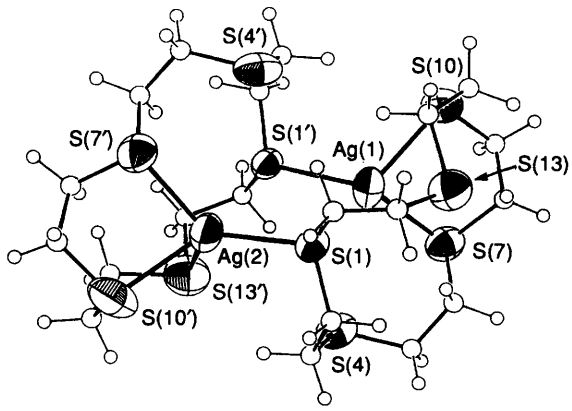

Fig. 1 View of the cation in $[Ag_2([15]aneS_5)_2][BPh_4]_2$ with the numbering scheme adopted

Ag(1)···S(1) 2.907(3) Å, giving an overall distorted tetrahedral environment at Ag. A different stereochemistry is observed at Ag(2) where co-ordination is through a [4 + 1] S-donor set involving three thioether donors of one macrocycle, Ag(2)–S(7′) 2.558(4), Ag(2)–S(10′) 2.623(5), Ag(2)–S(13′) 2.716(5) Å, one thioether donor of the other macrocycle, Ag(2)–S(1) 2.486(3) Å and a further long-range, weak interaction, Ag(2)···S(1′) 3.131(3) Å. The remaining S-donor atoms, S(4), S(13) and S(4′), are directed away from and do not interact with the metal centres, Ag(1)···S(4) 3.555(4), Ag(1)···S(13) 3.319(4), Ag(1)···S(4′) 3.994(4) Å. Notably therefore, S(1) and S(1′) act as asymmetric bridges between Ag(1) and Ag(2), giving a metal–metal distance of 4.2225(15) Å.

We have recently reported a related silver(I) complex incorporting a mixed thia/oxo donor macrocycle, $[Ag_n([15]aneS_2O_3)_n]^{n+}$, which shows a polymeric structure with bridging S-donors,[19] while Wieghardt and co-workers[16] have structurally characterised the unusual trimeric cation $[Ag_3([9]aneS_3)_3]^{3+}$. DeSimone and co-workers[20] have also reported the crystal structure of the dimolybdenum species $[Mo_2(SH)_2([16]aneS_4)_2]^{2+}$ {[16]aneS$_4$ = 1,5,9,13-tetrathiacyclohexadecane}. To our knowledge these are the only fully characterised examples to date which incorporate bridging thioether macrocyclic ligands. The paucity of such systems is not surprising since thioethers are generally very poor ligands for metal centres.[3] Thus the ability of thioether donors to function as asymmetrically bridging ligands in $[Ag_2([15]aneS_5)_2]^{2+}$ is quite remarkable, and serves to illustrate further how incorporation of the S(thioether) donors within a macrocyclic framework greatly enhances their ligating characteristics.

In view of the very unexpected stereochemical features observed for $[Ag_2([15]aneS_5)_2][BPh_4]_2$, we were intrigued as to whether replacement of the bulky organic BPh_4^- counter ion by the much smaller PF_6^- or the perfluorinated derivative of BPh_4^-, $[B(C_6F_5)_4]^-$, would significantly alter the structure of the resultant silver–thioether complex. Variation of counter ion has been shown previously to alter the structure of the cation in $[Pd([18]aneS_6)]^{2+}$.[1,21] We therefore undertook single crystal X-ray structure determinations on both the PF_6^- and $[B(C_6F_5)_4]^-$ salts of $[Ag([15]aneS_5)]^+$.

Colourless crystals of suitable quality were obtained by vapour diffusion of diethyl ether into a solution of $[Ag([15]aneS_5)]PF_6$ in $MeNO_2$. A single-crystal X-ray structure determination confirms the complex to have a completely different stereochemistry from that observed for $[Ag_2([15]aneS_5)_2][BPh_4]_2$. The structure of the PF_6^- salt shows (Fig. 2) two independent and antiparallel, infinite polymeric chains of $[Ag([15]aneS_5)]^+$ cations. Each silver(I) centre is bound *via* a [4 + 2] S-donor set in a distorted octahedral geometry. This donor set comprises three short and two long metal–thioether bonds to one [15]aneS$_5$ crown, Ag(1)-S(4) 2.659(5), Ag(1)-S(7) 2.651(6), Ag(1)-S(13) 2.564(6), Ag(1)···S(1) 3.219(5),

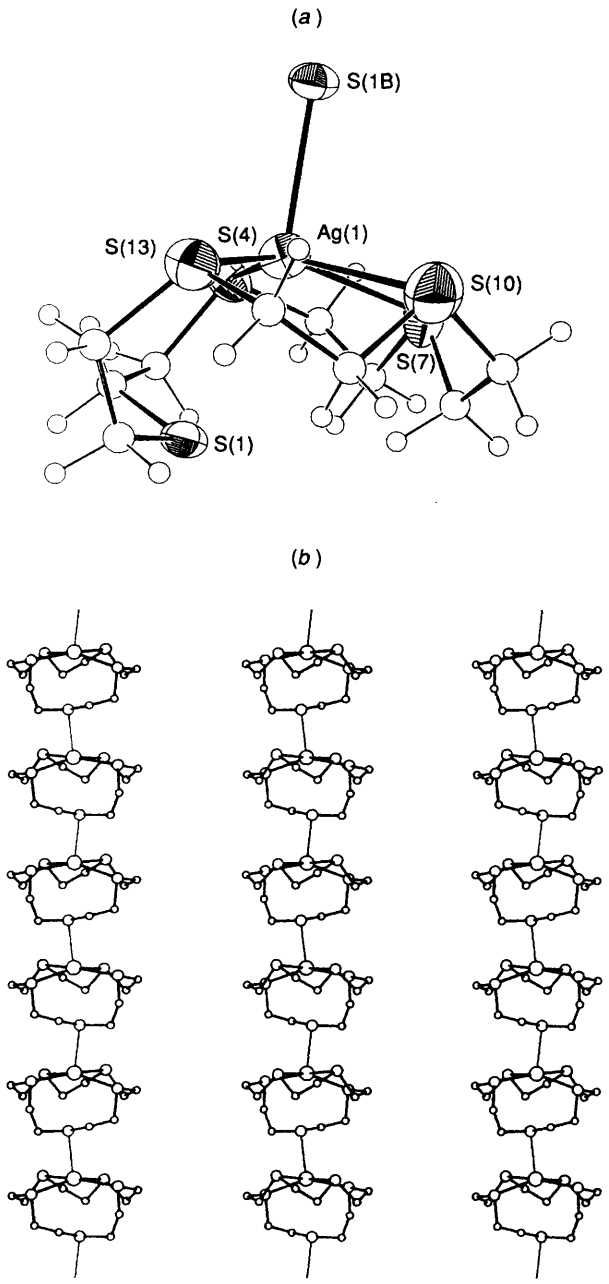

Fig. 2 (*a*) Illustration of the distorted octahedral co-ordination around Ag^{I} in $[Ag_n([15]aneS_5)_n][PF_6]_n$ with the numbering scheme adopted. (*b*) Packing diagram showing one of the arrangements of the polymeric $[Ag_n([15]aneS_5)_n]^{n+}$ chains in the PF_6^- salt (the other chains run antiparallel)

Ag(1)···S(10) 3.075(7) Å and one thioether donor from an adjacent macrocycle, Ag(1)–S(1B) 2.742(5) Å. A similar co-ordination sphere is observed at Ag(2), Ag(2)–S(4′) 2.605(5), Ag(2)–S(10′) 2.713(7), Ag(2)–S(13′) 2.637(6), Ag(2)···S(1′) 3.263(5), Ag(2)···S(7′) 2.964(8), Ag(2)–S(1D) 2.714(5) Å [S(1B) and S(1D) are related to S(1) and S(1′) by the symmetry operations $(x, -y, \frac{1}{2} + z)$ and $(-x, y, -\frac{1}{2} + z)$ respectively]. The $[Ag([15]aneS_5)]^+$ fragments are linked by S(1) and S(1′) which act as asymmetrically bridging donor atoms. This is similar to the polymeric structure observed for $[Ag_n([15]aneS_2O_3)_n]^{n+}$ in which the silver(I) ions are co-ordinated to a distorted octahedral $S_2O_3S_{bridge}$ donor set, Ag–S 2.5404(15), 2.7996(12), Ag–O 2.492(4), 2.667(5), 2.690(4), $Ag–S_{bridge}$ 2.5951(12) Å.[19]

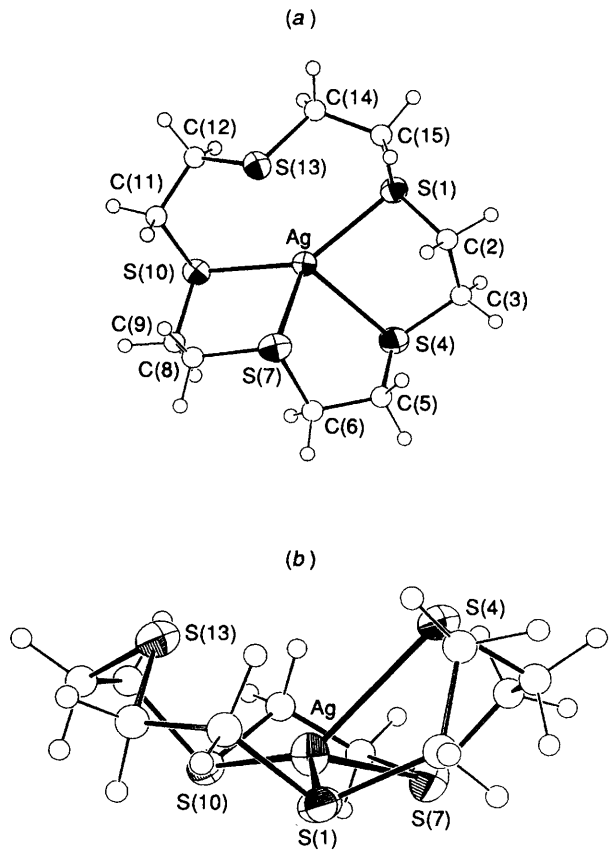

Fig. 3 Two views of the cation in $[Ag([15]aneS_5)][B(C_6F_5)_4]$ with the numbering scheme adopted

Single crystals of $[Ag([15]aneS_5)][B(C_6F_5)_4]$ were obtained by layering with hexane a solution of the complex in CH_2Cl_2. In contrast to the PF_6^- and BPh_4^- salts described above, this complex comprises discrete mononuclear $[Ag([15]aneS_5)]^+$ cations and $[B(C_6F_5)_4]^-$ anions. The structure shows (Fig. 3) Ag^{I} bound to all five S-donors of the crown in a very asymmetric [4 + 1] S-donor arrangement with Ag–S(1) 2.4712(19), Ag–S(4) 2.7262(20), Ag–S(7) 2.6847(21), Ag–S(10) 2.5621(19), Ag···S(13) 2.8813(19) Å. The primary S_4 co-ordination geometry is therefore distorted from a pseudo-tetrahedral arrangement by the long-range, secondary Ag···S(13) interaction, giving a formally five-co-ordinate silver(I) centre.

Thus, for the complexes $[Ag([15]aneS_5)]X$, changing the counter anion X leads to dramatic differences in the stereochemistry of the $[Ag([15]aneS_5)]^+$ cation, with significant changes in the number and nature of the Ag–S(thioether) interactions. From our previous work with related thioether macrocyclic complexes,[1] we believe that the restricted bite angle of the SCH_2CH_2S chelates within $[15]aneS_5$ plays an important role in determining the final structures of these silver(I) complexes. Additionally, the conformational flexibility of the crown thioether, and the absence of any crystal-field stabilisation energy for the d^{10} silver(I) ions, lead us to believe that crystal packing forces are also important in determining the overall solid-state structures. This is consistent with the observed structural trends upon altering the steric bulk of the counter anion. Carbon-13 NMR spectroscopic studies on the BPh_4^- and PF_6^- salts at 298 K in CD_3NO_2 show a single resonance for the methylene groups for each species at δ 31.26 and 31.59 respectively suggesting that these complexes do not retain their solid-state structures in solution. Thus, it appears that in solution the macrocyclic C atoms all experience the same environment. This may be due to time-averaging

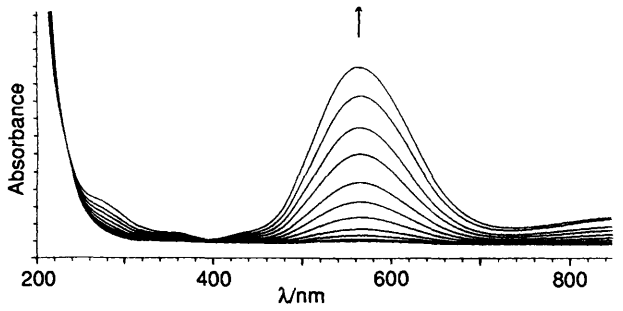

Fig. 4 *In situ* electronic spectrum for conversion of $[Ag([15]aneS_5)]^+$ into $[Ag([15]aneS_5)]^{2+}$ (OTE, 243 K, +1.5 V *vs.* $Ag–Ag^+$)

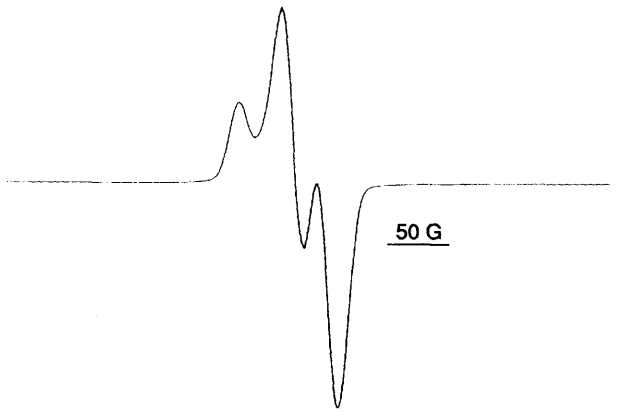

Fig. 5 X-Band ESR spectrum (77 K) of the oxidation product of $[Ag([15]aneS_5)]^+$ in H_2SO_4 glass

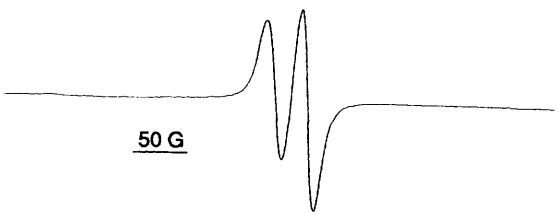

Fig. 6 X-Band ESR spectrum (298 K) of the oxidation product of $[Ag([15]aneS_5)]^+$ in H_2SO_4 solution

processes linked to the formation of solvated $[Ag([15]aneS_5)]^+$ monomers.

Cyclic voltammetry of $[Ag([15]aneS_5)]^+$ as its PF_6^- salt, measured at 298 K in MeCN (0.1 mol dm^{-3} $NBu^n_4PF_6$ supporting electrolyte) at platinum electrodes shows a chemically reversible oxidation at $E_{\frac{1}{2}} = +0.76$ V *vs.* ferrocene–ferrocenium and a quasi-reversible reduction at $E_{\frac{1}{2}} = -0.37$ V. Controlled-potential oxidation in MeCN at 243 K, +1.50 V *vs.* $Ag–Ag^+$, confirms that this is a single-electron process, generating an intense blue paramagnetic solution of the corresponding silver(II) species. The oxidation of $[Ag([15]aneS_5)]^+$ was monitored spectroelectrochemically by *in situ* electronic spectroscopy using an optically transparent electrode (OTE) system (Fig. 4). As expected, the original d^{10} silver(I) species shows no diagnostic electronic spectrum in the visible region. However, controlled electrochemical oxidation of the complex at 243 K in MeCN leads to growth of an intense absorption band ($\lambda_{max} = 565$ nm, $\varepsilon_{max} = 7700$ dm^3 mol^{-1} cm^{-1}). Electrochemical re-reduction of the oxidation product affords the starting spectrum; importantly, this demonstrates that interconversion of silver-(I) and -(II) species occurs reversibly at low temperatures. At room temperature the blue oxidation product is rapidly decolourised due to quenching of the radical species; this is consistent with the very powerful oxidising power of silver(II) species. The silver(II) species can also be

Table 1 X-Band ESR spectral data for oxidised silver thioether macrocyclic complexes (98% H_2SO_4)

Parent silver(I) complex	77 K	Solution (298 K)
$[Ag([9]aneS_3)_2]^+$	g_1 2.049	g_{iso} 2.034
	g_2 2.030	coupling not fully resolved
	g_3 2.009	
$[Ag([18]aneS_6)]^+$	g_1 2.054	g_{iso} 2.036
	g_2 2.029	A_{iso} 31 G
	g_3 2.010	
$[Ag([15]aneS_5)]^+$	g_1 2.043	g_{iso} 2.030
	g_2 2.020	A_{iso} 29 G
	g_3 2.009	
$[Ag([12]aneS_4)]^+$	g_1 2.055	g_{iso} 2.034
	g_2 2.036	A_{iso} 32 G
	g_3 2.014	
$[Ag([14]aneS_4)]^+$ *	g_1 2.044	g_{iso} 2.031
	g_2 2.035	A_{iso} 36 G
	g_3 2.007	
$[Ag([16]aneS_4)]^+$	g_1 2.056	g_{iso} 2.035
	g_2 2.037	A_{iso} 36 G
	g_3 2.010	

* $[14]aneS_4$ = 1,4,8,11-Tetrathiacyclotetradecane.

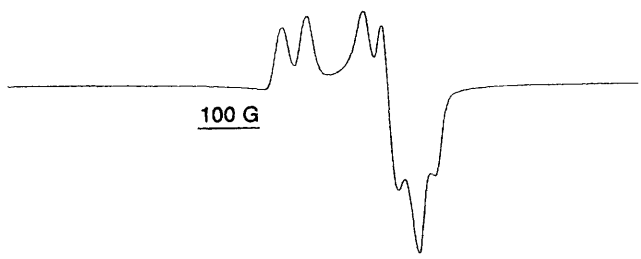

Fig. 7 Q-Band ESR spectrum (77 K) of the oxidation product of $[Ag([15]aneS_5)]^+$ in H_2SO_4 glass

generated chemically in 98% H_2SO_4 or 70% $HClO_4$,* and exhibits identical spectral features to electrochemically generated samples, confirming that we are observing the same species in these media.

The X-band ESR spectrum of the electrochemically generated silver(II) product (77 K, MeCN glass) shows a strong rhombic signal. Chemical oxidation (98% H_2SO_4 or 70% $HClO_4$*) generates the same species which shows a similar intense rhombic spectrum (Fig. 5). We have previously reported[12] similar ESR parameters for the oxidation products from related silver(I) octahedral thioether macrocyclic complexes. The solution X-band ESR spectrum (298 K, H_2SO_4) of the oxidation product from $[Ag([15]aneS_5)]^+$ shows (Fig. 6) a strong isotropic signal, $g_{iso} = 2.030$, which is clearly split into a doublet ($A_{iso} = 29$ G) by hyperfine coupling to ^{107}Ag ($I = \frac{1}{2}$) and ^{109}Ag ($I = \frac{1}{2}$), the couplings to both nuclei being very similar. Table 1 lists X-band ESR spectral data for a range of related silver-thioether macrocyclic complexes. Measurements at Q-band frequency (77 K, H_2SO_4 glass) revealed that the system has rhombic (or lower) ESR symmetry, $g_1 = 2.043$, $g_2 = 2.020$, $g_3 = 2.009$ and each g value has hyperfine splitting associated with it, $A_1 = 45.0$, $A_2 = 24.0$, $A_3 = 33.0$ G (Fig. 7). Thus, the lowest-field feature in the X-band spectra of the silver(II) complexes (Fig. 5) is the first silver hyperfine line for g_1. Both X- and Q-band spectra have been successfully simulated to give the reported g and A values (Fig. 8). The ESR spectral data suggest a high degree of covalency in the complexes with

* **CAUTION:** Perchloric acid and its salts are highly explosive particularly in the presence of organic materials. They should only be handled with utmost care.

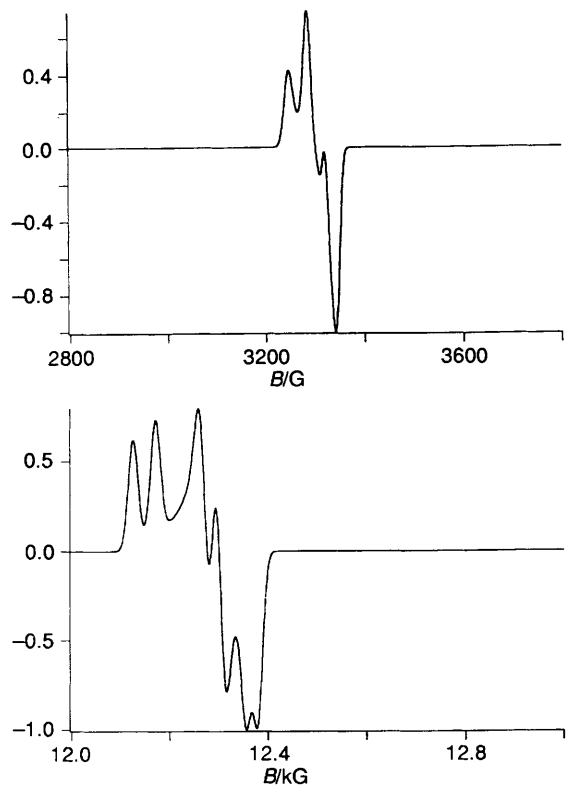

Fig. 8 Simulations of X- (top) and Q-band (bottom) ESR spectra (77 K) of oxidation products of $[Ag([15]aneS_5)]^+$

significant positive charge delocalised onto the S-donor atoms. This is reflected in the high instability, particularly in the solid state, of these oxidation products. We have therefore been unable thus far to confirm the assignment of these species as genuine silver(II) complexes by single-crystal X-ray diffraction.

Experimental

Infrared spectra were measured as KBr and CsI discs using a Perkin Elmer 598 spectrometer over the range 200–4000 cm^{-1}. Electrochemical measurements were performed on a Bruker E310 Universal Modular Polarograph. All readings were taken using a three-electrode potentiostatic system in acetonitrile containing 0.1 mol dm^{-3} $NBu^n_4PF_6$ or $NBu^n_4BF_4$ as supporting electrolyte. Cyclic voltammetric measurements were carried out using a double platinum electrode and a Ag–AgCl reference electrode. All potentials are quoted *versus* ferrocene–ferrocenium. The UV/VIS spectra were measured in quartz cells using a Perkin Elmer Lambda 9 spectrophotometer. Spectroelectrochemical measurements were carried out in quartz cells (pathlength 0.5 mm) fitted with a fine platinum–rhodium gauze as a working electrode. The platinum auxiliary electrode and $Ag–Ag^+$ reference electrode were fitted into a quartz extension attached to the cell, and were protected from the bulk solution by porous glass frits. The temperature of the cell was maintained using a thermocouple and digital thermometer. Microanalyses were performed by the Edinburgh University Chemistry Department microanalytical service. The ESR spectra were recorded as solutions or as frozen glasses down to 77 K using a Bruker ER200D X-band spectrometer and Varian E112 Q-band spectrometer. Simulations were performed on the Amdahl 5890–300E computer at Manchester Computing Centre using methods described previously.[22] Mass spectra were run by electron impact on a Kratos MS902 and by fast-atom bombardment (FAB) (3-nitrobenzyl alcohol matrix) on a Kratos MS 50TC spectrometer. Proton and ^{13}C NMR spectra were obtained on Bruker WP80 and WP200 instruments.

(*a*) *Synthesis of* $[Ag_n([15]aneS_5)_n][PF_6]_n$.—To a refluxing solution of $[15]aneS_5$ (85 mg, 0.283 mmol) in water–MeOH (1:1 v/v, 20 cm^3) was added 1 molar equivalent of $AgNO_3$ (50 mg, 0.294 mmol). The reaction mixture was refluxed for *ca.* 30 min, cooled and filtered into a solution containing an excess of NH_4PF_6 in water, to give a white precipitate. Recrystallisation from $MeNO_2$–Et_2O afforded a light-sensitive white solid (yield 75%) (Found: C, 20.9; H, 3.55; S, 28.9. Calc. for $C_{10}H_{20}AgF_6PS_5$: C, 21.7; H, 3.65; S, 29.0%). FAB mass spectrum: M^+ at m/z = 409, 407; calc. for $[^{109}Ag([15]aneS_5)]^+$ m/z 409, $[^{107}Ag([15]aneS_5)]^+$ m/z = 407. NMR (CD_3NO_2, 298 K): ^1H (200.13 MHz), δ 3.07 (CH_2, 20 H); ^{13}C DEPT (distortionless enhancement polarisation transfer) (50.32 MHz), δ 31.59 (CH_2). IR (KBr disc): 2980w, 2910m, 2820w, 1425vs, 1415vs, 1380w, 1295m, 1260m, 1250m, 1190m, 1170w, 1150w, 1130w, 1010w, 995w, 935m, 920m, 840vs, 740w, 690w, 640w, 555vs, 470w, 445w, 430w, 410w cm^{-1}.

(*b*) *Structure Determination of* $[Ag_n([15]aneS_5)_n][PF_6]_n$ **1**.—*Data collection and processing.* Stoë STADI-4 four-circle diffractometer, graphite-monochromated Mo-Kα X-radiation, ω–2θ scans using the learnt-profile method,[23] semiempirical absorption correction applied (minimum 0.3549, maximum 0.4810) by means of ψ-scans.

Structure solution and refinement. The data showed a clear tetragonal sub-cell [space group $P\bar{4}2_1m$, a = 18.194, c = 5.850 Å, 792 unique data, 772 reflections used with $F > 6\sigma(F)$] and only the data fitting this cell were used initially. The Ag atom was located by a Patterson synthesis. Iterative cycles of least-squares refinement and Fourier difference syntheses located all non-H atoms.[24] However, disorder was identified in all of the methylene C atoms and the F atoms. The structure was refined to R = 0.090, R' = 0.0985. At this stage the silver position was transferred into the true orthorhombic I cell giving two independent $[Ag([15]aneS_5)]^+PF_6^-$ ion pairs per unit cell [transformation: new coordinates $x = \frac{1}{2}(x - y) + 0.25$, $y = \frac{1}{2}(x + y) - 0.25$, $z = \frac{z}{2}$; $x' = \frac{1}{2}(x + y) + 0.25$; $y' = \frac{1}{2}(y - x) - 0.25$, $z' = -\frac{z}{2}$]. The origin was fixed by constraining the sum of the z parameters for the two silver atoms to be 2.0. All other non-H atoms were then located by successive least-squares refinement and Fourier difference syntheses.[24] Some disorder was identified in one of the PF_6^- anions. This was modelled successfully using partial occupancies giving two orientations: 66.7% with a C_2 axis though the P atom, with three general F atoms, and 33.3% with a C_2 axis coincident with the F–P–F axis, with two general F atoms. All C–C and C–S bonds in the $[15]aneS_5$ macrocycle were constrained to be 1.50(1) and 1.83(1) Å respectively. Anisotropic thermal parameters were refined for Ag, S, P and all F atoms with occupancies $\geqslant \frac{2}{3}$. Hydrogen atoms were included in fixed, calculated positions.[25]

Crystallographic data are given in Table 2, bond lengths, angles and torsion angles in Table 3 and fractional atomic coordinates in Table 4.

(*c*) *Synthesis of* $[Ag_2([15]aneS_5)_2][BPh_4]_2$.—Procedure as for (*a*) above, but using $NaBPh_4$ in place of NH_4PF_6. Yield 72% (Found: C, 56.0; H, 5.50; S, 22.4. Calc. for $C_{34}H_{40}AgBS_5$: C, 56.1; H, 5.55; S, 22.0%). FAB mass spectrum: M^+ at m/z 407, 409; calc. for $[^{107}Ag([15]aneS_5)]^+$ m/z = 407, $[^{109}Ag([15]aneS_5)]^+$ m/z = 409. NMR (CD_3NO_2, 298 K): ^1H (200.13 MHz), 7.38–6.80 (m, phenyl CH, 20 H), 3.01 (s, CH_2, 20 H); ^{13}C DEPT (50.32 MHz), δ 134.76, 124.67, 120.81 (all phenyl CH), 31.26 (CH_2). IR (KBr disc): 3040w, 3020w, 2980w, 2910m, 1580m, 1475m, 1420m, 1410m, 1260m, 1170w, 1130w, 1060w, 1030w, 920w, 840w, 740vs, 710vs, 610m, 470w cm^{-1}.

(*d*) *Structure Determination of* $[Ag_2([15]aneS_5)_2][BPh_4]_2$ **2**.—*Data collection and processing.* Details as for complex **1**, except for limiting values in semiempirical absorption correction (minimum 0.2301, maximum 0.3226).

Structure solution and refinement. The Ag atoms were

Table 2 Crystal data and details of data collection and structure refinement

	1	2	3
Formula	$C_{10}H_{20}AgF_6PS_5$	$C_{68}H_{80}Ag_2B_2S_{10}$	$C_{34}H_{20}AgBF_{20}S_5 \cdot 2.5CH_2Cl_2$
M	553.3	1455.3	1299.6
Crystal size (mm)	0.38 × 0.54 × 0.59	0.19 × 0.27 × 0.69	0.19 × 0.19 × 0.31
Crystal system	Orthorhombic	Triclinic	Triclinic
Space group	*Iba*2	$P\bar{1}$	$P\bar{1}$
a/Å	25.713(3)	11.462(3)	12.476(5)
b/Å	25.749(3)	11.895(3)	13.658(7)
c/Å	11.6989(19)	27.019(10)	15.608(6)
α/°	90	78.503(18)	108.300(22)
β/°	90	84.729(13)	108.467(17)
γ/°	90	67.118(18)	100.518(21)
U/Å^3	7746	3325	2275
D_c/g cm^{-3}	1.898	1.453	1.897
Z	16	2	2
μ/mm^{-1}	1.675	1.453	1.066
$F(000)$	4416	1504	1282
T/K	298	298	150
Reflections at $\pm\omega$ to refine cell	48	18	23
2θ range/°	24.5–25.1	31–32	25–26
$2\theta_{max}$/°	45	45	45
h, k, l ranges	0–27, 0–27, 0–12	−12 to 12, −12 to 12, 0–27	−13 to 12, −14 to 13, 0–16
Reflections measured			
Total	3134	8627	6175
Unique	2668	7925	5497
Observed [$F \geqslant 4\sigma(F)$]			4693
Observed [$F \geqslant 6\sigma(F)$]	2473	6344	
Parameters refined	326	634	576
Weighting scheme, g in $w^{-1} = \sigma^2(F) + gF^2$	0.000 024	0.000 086	0.000 103
R, R'	0.0597, 0.0719	0.0859, 0.1108	0.0493, 0.0588
S	1.414	1.117	1.093
Max. and min. residues in final ΔF synthesis (e Å^{-3})	+0.66 −0.58	+2.15 −1.17	+0.83 −0.87

Table 3 Bond lengths (Å), angles and torsion angles (°) with estimated standard deviations (e.s.d.s) for $[Ag_n([15]aneS_5)_n][PF_6]_n$

Ag(1) · · · S(1)	3.219(5)	Ag(2) · · · S(1′)	3.263(5)
Ag(1)–S(4)	2.659(5)	Ag(2)–S(4′)	2.605(5)
Ag(1)–S(7)	2.651(6)	Ag(2) · · · S(7′)	2.964(8)
Ag(1) · · · S(10)	3.075(7)	Ag(2)–S(10′)	2.713(7)
Ag(1)–S(13)	2.564(6)	Ag(2)–S(13′)	2.637(6)
Ag(1)–S(1B)	2.742(5)	Ag(2)–S(1D)	2.714(5)
S(4)–Ag(1)–S(7)	79.79(18)	Ag(1)–S(13)–C(14)	111.5(6)
S(4)–Ag(1)–S(13)	127.70(17)	C(12)–S(13)–C(14)	106.9(9)
S(4)–Ag(1)–S(1B)	99.64(16)	S(13)–C(14)–C(15)	117.1(12)
S(7)–Ag(1)–S(13)	141.82(19)	S(1)–C(15)–C(14)	116.3(11)
S(7)–Ag(1)–S(1B)	101.34(18)	C(2′)–S(1′)–C(15′)	102.6(8)
S(13)–Ag(1)–S(1B)	99.17(16)	S(1′)–C(2′)–C(3′)	106.6(13)
S(4′)–Ag(2)–S(10′)	141.18(20)	C(2′)–C(3′)–S(4′)	115.2(13)
S(4′)–Ag(2)–S(13′)	126.83(18)	Ag(2)–S(4′)–C(3′)	109.3(6)
S(4′)–Ag(2)–S(1D)	99.64(16)	Ag(2)–S(4′)–C(5′)	105.0(6)
S(10′)–Ag(2)–S(13′)	78.65(20)	C(3′)–S(4′)–C(5′)	104.5(9)
S(10′)–Ag(2)–S(1D)	103.76(19)	S(4′)–C(5′)–C(6′)	117.0(14)
S(13′)–Ag(2)–S(1D)	100.35(17)	C(5′)–C(6′)–S(7′)	107.6(13)
C(2)–S(1)–C(15)	102.1(8)	C(6′)–S(7′)–C(8′)	101.4(10)
S(1)–C(2)–C(3)	111.8(13)	S(7′)–C(8′)–C(9′)	114.4(15)
C(2)–C(3)–C(4)	112.7(13)	C(8′)–C(9′)–S(10′)	108.9(14)
Ag(1)–S(4)–C(3)	109.5(6)	Ag(2)–S(10′)–C(9′)	97.0(7)
Ag(1)–S(4)–C(5)	101.1(6)	Ag(2)–S(10′)–C(11′)	96.7(6)
C(3)–S(4)–C(5)	102.6(9)	C(9′)–S(10′)–C(11′)	96.0(9)
S(4)–C(5)–C(6)	116.2(13)	S(10′)–C(11′)–C(12′)	106.7(12)
C(5)–C(6)–S(7)	106.6(12)	C(11′)–C(12′)–S(13′)	115.1(13)
Ag(1)–S(7)–C(6)	99.3(6)	Ag(2)–S(13′)–C(12′)	103.2(6)
Ag(1)–S(7)–C(8)	99.8(6)	Ag(2)–S(13′)–C(14′)	113.1(6)
C(6)–S(7)–C(8)	95.7(8)	C(12′)–S(13′)–C(14′)	105.7(9)
S(7)–C(8)–C(9)	107.2(12)	S(13′)–C(14′)–C(15′)	117.3(13)
C(8)–C(9)–S(10)	116.0(13)	S(1′)–C(15′)–C(14′)	118.0(13)
C(9)–S(10)–C(11)	105.6(9)	Ag(1)–S(1B)–C(2B)	104.7(6)
S(10)–C(11)–C(12)	109.9(13)	Ag(1)–S(1B)–C(15B)	98.2(5)
C(11)–C(12)–S(13)	114.6(13)	Ag(2)–S(1D)–C(2D)	102.0(6)
Ag(1)–S(13)–C(12)	108.5(6)	Ag(2)–S(1D)–C(15D)	99.4(5)

Table 3 (*continued*)

C(15)–S(1)–C(2)–C(3)	168.4(13)	C(15′)–S(1′)–C(2′)–C(3′)	−167.0(12)
C(2)–S(1)–C(15)–C(14)	−59.8(14)	C(2′)–S(1′)–C(15′)–C(14′)	63.5(15)
S(1)–C(2)–C(3)–S(4)	−75.1(14)	S(1′)–C(2′)–C(3′)–S(4′)	78.6(14)
C(2)–C(3)–S(4)–C(5)	130.6(13)	C(2′)–C(3′)–S(4′)–C(5′)	−143.4(14)
C(3)–S(4)–C(5)–C(6)	−77.4(15)	C(3′)–S(4′)–C(5′)–C(6′)	82.4(16)
S(4)–C(5)–C(6)–S(7)	−68.2(15)	S(4′)–C(5′)–C(6′)–S(7′)	72.0(16)
C(5)–C(6)–S(7)–C(8)	160.5(12)	C(5′)–C(6′)–S(7′)–C(8′)	−164.9(14)
C(6)–S(7)–C(8)–C(9)	−177.1(12)	C(6′)–S(7′)–C(8′)–C(9′)	82.4(16)
S(7)–C(8)–C(9)–S(10)	61.6(15)	S(7′)–C(8′)–C(9′)–S(10′)	59.1(17)
C(8)–C(9)–S(10)–C(11)	73.6(15)	C(8′)–C(9′)–S(10′)–C(11′)	−173.0(14)
C(9)–S(10)–C(11)–C(12)	−165.0(13)	C(9′)–S(10′)–C(11′)–C(12′)	160.9(13)
S(10)–C(11)–C(12)–S(13)	71.5(15)	S(10′)–C(11′)–C(12′)–S(13′)	−68.6(15)
C(11)–C(12)–S(13)–C(14)	95.3(15)	C(11′)–C(12′)–S(13′)–C(14′)	−86.9(15)
C(12)–S(13)–C(14)–C(15)	−64.6(15)	C(12′)–S(13′)–C(14′)–C(15′)	61.5(15)
S(13)–C(14)–C(15)–S(1)	−55.4(16)	S(13′)–C(14′)–C(15′)–S(1′)	51.4(18)

Table 4 Atomic coordinates with e.s.d.s for $[Ag_n([15]aneS_5)_n][PF_6]_n$

Atom	*x*	*y*	*z*	Atom	*x*	*y*	*z*
Ag(1)	0.196 35(5)	0.002 05(6)	1.053 45(9)	F(33)	0.039 7(9)	0.507 7(9)	0.845 4(24)
Ag(2)	0.000 65(6)	0.304 36(5)	0.946 55(9)	C(2)	0.118 1(5)	0.025 9(5)	0.807 3(23)
S(1)	0.177 36(18)	−0.011 45(17)	0.783 2(5)	C(3)	0.129 6(8)	0.081 4(6)	0.834 5(11)
S(4)	0.154 08(20)	0.090 23(17)	0.980 3(5)	C(5)	0.212 1(5)	0.130 2(6)	0.958 0(22)
S(7)	0.280 98(19)	0.059 91(21)	1.030 3(7)	C(6)	0.259 1(7)	0.102 6(7)	0.915 0(14)
S(10)	0.293 09(22)	−0.066 75(23)	1.083 9(6)	C(8)	0.319 9(7)	0.017 1(6)	0.939 1(14)
S(13)	0.162 66(20)	−0.090 61(19)	1.022 7(5)	C(9)	0.341 2(6)	−0.025 2(7)	1.014 0(19)
S(1′)	−0.012 19(16)	0.324 74(18)	1.220 4(5)	C(11)	0.267 2(7)	−0.108 5(7)	0.971 1(14)
S(4′)	0.090 42(17)	0.336 82(20)	1.021 1(5)	C(12)	0.218 1(5)	−0.134 0(6)	1.011 0(21)
S(7′)	0.065 77(24)	0.209 63(25)	0.931 8(9)	C(14)	0.126 3(6)	−0.096 1(8)	0.889 9(11)
S(10′)	−0.062 16(25)	0.219 73(23)	0.950 7(7)	C(15)	0.152 9(7)	−0.078 2(4)	0.782 9(15)
S(13′)	−0.090 81(20)	0.347 35(23)	0.984 3(5)	C(2′)	0.031 8(5)	0.379 9(5)	1.200 4(23)
P(1)	0.248 79(22)	0.259 12(20)	0.750 3(5)	C(3′)	0.083 8(7)	0.357 7(9)	1.169 4(11)
F(11)	0.250 0(5)	0.261 1(5)	0.618 9(10)	C(5′)	0.130 9(6)	0.278 7(5)	1.028 4(22)
F(12)	0.246 4(6)	0.257 6(5)	0.885 2(11)	C(6′)	0.104 2(8)	0.228 8(7)	1.056 7(15)
F(13)	0.198 2(5)	0.225 1(6)	0.746 7(16)	C(8′)	0.023 2(8)	0.160 2(7)	0.993 3(22)
F(14)	0.216 6(7)	0.309 4(5)	0.751 5(14)	C(9′)	−0.023 7(7)	0.181 4(8)	1.053 2(15)
F(15)	0.301 8(6)	0.291 3(6)	0.756 4(14)	C(11′)	−0.108 6(7)	0.244 9(7)	1.055 6(15)
F(16)	0.282 0(5)	0.206 6(5)	0.747 8(15)	C(12′)	−0.133 6(6)	0.291 6(6)	1.002 8(21)
P(2)	0.000 0	0.000 0	0.564 5(7)	C(14′)	−0.093 7(8)	0.383 1(7)	1.118 4(11)
F(21)	−0.000 1(12)	−0.039 9(7)	0.464 1(15)	C(15′)	−0.075 7(5)	0.355 6(8)	1.223 4(17)
F(22)	−0.059 3(4)	0.009 5(13)	0.562 3(22)	F(24)	−0.045 8(11)	−0.038 7(12)	0.568(4)
F(23)	0.007 4(12)	0.043 0(9)	0.656 2(23)	F(25)	−0.029(4)	0.052 6(23)	0.550(12)
P(3)	0.000 0	0.500 0	0.930 4(8)	F(26)	0.000 0	0.000 0	0.697 0(11)
F(31)	0.017 5(7)	0.443 2(4)	0.932 3(17)	F(27)	0.000 0	0.000 0	0.432 2211)
F(32)	−0.040 1(7)	0.495 2(9)	1.030 3(22)				

located by a Patterson synthesis and the structure was developed by least-squares refinement and Fourier difference syntheses.[24] During refinement some disorder in the macrocyclic methylene groups was identified. This was modelled using partial C atoms, giving two equally likely sites for C(11′) and C(12′). These, together with the other C atoms, C(12) and C(14′), exhibiting high thermal parameters were refined isotropically, and the C–C and C–S bond lengths in the regions S(7) to S(13) and S(7′) to S(13′) were constrained to be 1.50 and 1.83 Å respectively. All other non-H atoms were refined anisotropically. At isotropic convergence final corrections (minimum 0.691, maximum 1.146) for absorption effects were applied using DIFABS.[26] Hydrogen atoms were included in fixed, calculated positions and the phenyl groups of the BPh_4^- counter ions were refined as rigid groups.

Selected bond lengths, angles and torsion angles are given in Table 5, fractional atomic coordinates in Table 6.

(*e*) *Synthesis of* $[Ag([15]aneS_5)][B(C_6F_5)_4]$.—Procedure as for (*a*) above, but using $Li[B(C_6F_5)_4]$ in place of NH_4PF_6. Yield 72% (Found: C, 37.6; H, 1.85. Calc. for $C_{34}H_{20}AgBF_{20}S_5$: C, 37.5; H, 2.10%). FAB mass spectrum: M^+ at *m*/*z* 407, 409; calc. for $[^{107}Ag([15]aneS_5)]^+$ *m*/*z* = 407, $[^{109}Ag([15]aneS_5)]^+$ *m*/*z* = 409. IR (KBr disc): 2950w, 2920m, 2845w, 1640s, 1600w, 1510vs, 1475vs, 1430m, 1410m, 1380m, 1370m, 1300w, 1265s, 1090vs, 1030w, 975vs, 930w, 915w, 870w, 855w, 840w, 825w, 770vs, 765m, 755vs, 745w, 735m, 725m, 680vs, 660vs, 645w, 610m, 600m, 570m, 470w cm^{-1}.

(*f*) *Structure Determination of* $[Ag([15]aneS_5)][B(C_6F_5)_4]$ **3**.—*Data collection and processing.* Details as for complex **1**, except that data were collected at 150K rather than 298K, the crystal being cooled using an Oxford Cryosystems low-temperature device[27] and no absorption correction was applied at this stage.

Structure solution and refinement. An Ag atom was located by a Patterson synthesis and the structure was developed by least-squares refinement and Fourier difference syntheses.[24] During refinement some disorder in the macrocyclic methylene groups was identified. This was modelled using partial C atoms, giving two alternative sites for C(8) and C(9) [C(8) and C(9) 62% occupied, C(8′) and C(9′) 38% occupied]. These, together with the other C atoms, C(12) and C(14′), exhibiting high thermal parameters were refined isotropically, and the C–C and C–S

Table 5 Bond lengths (Å), angles and torsion angles (°) with e.s.d.s for $[Ag_2([15]aneS_5)_2][BPh_4]_2$

Ag(1)···Ag(2)	4.2225(15)	C(14)–C(15)	1.421(18)
Ag(1)···S(1)	2.907(3)	Ag(2)···S(1′)	3.131(3)
Ag(1)···S(4)	3.555(4)	Ag(2)···S(4′)	3.994(4)
Ag(1)–S(7)	2.529(3)	Ag(2)–S(7′)	2.558(4)
Ag(1)–S(10)	2.608(4)	Ag(2)–S(10′)	2.623(5)
Ag(1)···S(13)	3.319(4)	Ag(2)–S(13′)	2.716(5)
Ag(1)–S(1′)	2.537(3)	S(1′)–C(2′)	1.814(11)
S(1)–C(2)	1.818(11)	S(1′)–C(15′)	1.848(12)
S(1)–C(15)	1.821(13)	C(2′)–C(3′)	1.477(17)
S(1)–Ag(2)	2.486(3)	C(3′)–S(4′)	1.802(13)
C(2)–C(3)	1.520(16)	S(4′)–C(5′)	1.805(14)
C(3)–S(4)	1.817(12)	C(5′)–C(6′)	1.493(19)
S(4)–C(5)	1.813(12)	C(6′)–S(7′)	1.802(13)
C(5)–C(6)	1.516(17)	S(13′)–C(14′)	1.868(14)
C(6)–S(7)	1.807(13)		
S(1)–Ag(1)–S(7)	112.53(10)	Ag(1)–S(1′)–Ag(2)	95.76(9)
S(1)–Ag(1)–S(10)	132.46(11)	Ag(1)–S(1′)–C(2′)	111.3(4)
S(1)–Ag(1)–S(1′)	82.40(8)	Ag(1)–S(1′)–C(15′)	115.1(4)
S(7)–Ag(1)–S(10)	85.20(12)	Ag(2)–S(1′)–C(2′)	127.8(4)
S(7)–Ag(1)–S(1′)	135.90(11)	Ag(2)–S(1′)–C(15′)	104.6(4)
S(10)–Ag(1)–S(1′)	115.87(11)	C(2′)–S(1′)–C(15′)	102.8(5)
C(2)–S(1)–C(15)	102.0(5)	S(1′)–C(2′)–C(3′)	111.3(8)
C(2)–S(1)–Ag(2)	111.7(4)	C(2′)–C(3′)–S(4′)	117.8(9)
C(15)–S(1)–Ag(2)	112.0(4)	C(3′)–S(4′)–C(5′)	103.1(6)
S(1)–C(2)–C(3)	109.6(8)	S(4′)–C(5′)–C(6′)	115.8(10)
C(2)–C(3)–S(4)	116.6(8)	C(5′)–C(6′)–S(7′)	109.6(9)
C(3)–S(4)–C(5)	104.3(6)	Ag(2)–S(7′)–C(6′)	109.2(4)
S(4)–C(5)–C(6)	116.6(9)	Ag(2)–S(7′)–C(8′)	95.2(5)
C(5)–C(6)–S(7)	110.8(9)	C(6′)–S(7′)–C(8′)	94.4(6)
Ag(1)–S(7)–C(6)	102.6(4)	S(7′)–C(8′)–C(9′)	108.5(10)
Ag(1)–S(7)–C(8)	94.6(3)	C(8′)–C(9′)–S(10′)	114.6(11)
C(6)–S(7)–C(8)	101.2(5)	Ag(2)–S(10′)–C(9′)	99.6(5)
Ag(1)–S(10)–C(9)	96.9(3)	Ag(2)–S(10′)–C(11′)	104.5(6)
Ag(1)–S(10)–C(11)	107.1(3)	Ag(2)–S(10′)–C(11D)	103.5(7)
C(9)–S(10)–C(11)	111.9(4)	C(9′)–S(10′)–C(11′)	101.2(8)
C(12)–S(13)–C(14)	98.7(5)	C(9′)–S(10′)–C(11D)	122.7(9)
S(13)–C(14)–C(15)	120.8(9)	S(10′)–C(11′)–C(12′)	109.2(12)
S(1)–C(15)–C(14)	116.1(9)	C(11′)–C(12′)–S(13′)	109.1(11)
S(1)–Ag(2)–S(1′)	78.71(8)	Ag(2)–S(13′)–C(12′)	91.7(5)
S(1)–Ag(2)–S(7′)	125.68(11)	Ag(2)–S(13′)–C(14′)	107.3(5)
S(1)–Ag(2)–S(10′)	131.25(12)	Ag(2)–S(13′)–C(12D)	100.8(6)
S(1)–Ag(2)–S(13′)	110.16(12)	C(12′)–S(13′)–C(14′)	91.8(6)
S(1′)–Ag(2)–S(7′)	97.10(10)	C(14′)–S(13′)–C(12D)	108.0(8)
S(1′)–Ag(2)–S(10′)	142.82(12)	S(13′)–C(14′)–C(15′)	107.9(9)
S(1′)–Ag(2)–S(13′)	68.95(11)	S(1′)–C(15′)–C(14′)	110.5(8)
S(7′)–Ag(2)–S(10′)	82.40(13)	S(10′)–C(11D)–C(12D)	109.1(14)
S(7′)–Ag(2)–S(13′)	118.61(13)	S(13′)–C(12D)–C(11D)	109.1(14)
S(10′)–Ag(2)–S(13′)	78.68(14)		
C(15)–S(1)–C(2)–C(3)	173.3(8)	C(2′)–C(3′)–S(4′)–C(5′)	−69.2(10)
C(2)–S(1)–C(15)–C(14)	68.5(10)	C(3′)–S(4′)–C(5′)–C(6′)	88.3(11)
S(1)–C(2)–C(3)–S(4)	55.9(10)	S(4′)–C(5′)–C(6′)–S(7′)	66.1(11)
C(2)–C(3)–S(4)–C(5)	70.0(10)	C(5′)–C(6′)–S(7′)–C(8′)	164.8(10)
C(3)–S(4)–C(5)–C(6)	−94.6(10)	C(6′)–S(7′)–C(8′)–C(9′)	174.4(10)
S(4)–C(5)–C(6)–S(7)	−59.2(11)	S(7′)–C(8′)–C(9′)–S(10′)	−67.5(12)
C(5)–C(6)–S(7)–C(8)	−174.6(8)	C(8′)–C(9′)–S(10′)–C(11′)	−78.2(12)
C(6)–S(7)–C(8)–C(9)	−164.9(6)	C(8′)–C(9′)–S(10′)–C(11D)	−84.2(14)
S(7)–C(8)–C(9)–S(10)	78.5(6)	C(9′)–S(10′)–C(11′)–C(12′)	74.4(12)
C(8)–C(9)–S(10)–C(11)	66.5(6)	C(9′)–S(10′)–C(11D)–C(12D)	59.8(17)
C(9)–S(10)–C(11)–C(12)	−120.5(6)	S(10′)–C(11′)–C(12′)–S(13′)	72.4(12)
S(10)–C(11)–C(12)–S(13)	84.5(6)	C(11′)–C(12′)–S(13′)–C(14′)	−178.2(11)
C(11)–C(12)–S(13)–C(14)	174.5(7)	C(12′)–S(13′)–C(14′)–C(15′)	162.9(9)
C(12)–S(13)–C(14)–C(15)	66.8(11)	C(12D)–S(13′)–C(14′)–C(15′)	178.4(10)
S(13)–C(14)–C(15)–S(1)	42.6(13)	C(14′)–S(13′)–C(12D)–C(11D)	−164.1(13)
C(15′)–S(1′)–C(2′)–C(3′)	−176.6(8)	S(13′)–C(14′)–C(15′)–S(1′)	−66.0(10)
C(2′)–S(1′)–C(15′)–C(14′)	−103.8(9)	S(10′)–C(11D)–C(12D)–S(13′)	72.4(15)
S(1′)–C(2′)–C(3′)–S(4′)	−48.7(11)		

bond lengths in the regions S(7) to S(13) and S(7′) to S(13′) were constrained to be 1.50 and 1.83 Å respectively. At isotropic convergence corrections (minimum 0.840, maximum 1.231) for absorption effects were applied using DIFABS.[26] All fully occupied non-H atoms were refined anisotropically. A peak *ca.* 1.3 Å from Ag refined as a fragment of another silver ion with

Table 6 Atomic coordinates with e.s.d.s for $[Ag_2([15]aneS_5)_2][BPh_4]_2$

Atom	*x*	*y*	*z*	Atom	*x*	*y*	*z*
Ag(1)	0.766 90(10)	0.074 96(9)	0.679 49(4)	C(14R)	0.273 4(5)	0.560 8(5)	0.605 82(22)
S(1)	0.566 02(23)	0.102 98(22)	0.755 63(10)	C(15R)	0.196 9(5)	0.506 6(5)	0.591 14(22)
C(2)	0.483 9(9)	0.255 3(9)	0.772 6(4)	C(16R)	0.077 6(5)	0.581 1(5)	0.571 32(22)
C(3)	0.575 4(10)	0.290 1(10)	0.797 7(4)	C(17R)	0.034 8(5)	0.709 8(5)	0.566 15(22)
S(4)	0.718 4(3)	0.288 0(3)	0.760 07(13)	C(18R)	0.111 3(5)	0.763 9(5)	0.580 81(22)
C(5)	0.663 1(11)	0.418 7(9)	0.710 6(5)	C(19R)	0.468 7(4)	0.697 4(5)	0.589 73(20)
C(6)	0.637 3(10)	0.391 2(10)	0.661 2(5)	C(20R)	0.478 6(4)	0.655 4(5)	0.544 28(20)
S(7)	0.778 6(3)	0.280 2(3)	0.637 31(12)	C(21R)	0.594 6(4)	0.618 2(5)	0.518 43(20)
C(8)	0.724 8(9)	0.277 1(3)	0.576 07(20)	C(22R)	0.700 6(4)	0.623 1(5)	0.538 00(20)
C(9)	0.816 7(10)	0.165 9(6)	0.556 12(17)	C(23R)	0.690 7(4)	0.665 2(5)	0.583 45(20)
S(10)	0.788 1(3)	0.027 9(3)	0.588 10(14)	C(24R)	0.574 7(4)	0.702 3(5)	0.609 32(20)
C(11)	0.634 2(4)	0.033 1(9)	0.572 1(3)	B(2)	0.122 8(10)	0.252 3(9)	0.878 0(4)
S(13)	0.476 6(4)	0.183 2(3)	0.634 22(14)	C(25R)	0.181 9(6)	0.096 0(4)	0.895 59(21)
C(14)	0.379 7(11)	0.148 2(13)	0.688 1(3)	C(26R)	0.134 7(6)	0.038 0(4)	0.938 08(21)
C(15)	0.436 8(10)	0.072 9(11)	0.734 0(4)	C(27R)	0.187 7(6)	−0.090 6(4)	0.952 47(21)
Ag(2)	0.675 28(10)	−0.054 73(8)	0.829 16(4)	C(28R)	0.287 9(6)	−0.161 4(4)	0.924 36(21)
S(1′)	0.890 84(23)	−0.104 35(22)	0.746 65(10)	C(29R)	0.335 1(6)	−0.103 4(4)	0.881 87(21)
C(2′)	0.970 9(9)	−0.245 1(9)	0.720 7(4)	C(30R)	0.282 1(6)	0.025 3(4)	0.867 49(21)
C(3′)	0.882 0(11)	−0.273 1(10)	0.693 8(5)	C(31R)	0.105 5(6)	0.286 4(5)	0.814 19(15)
S(4′)	0.735 4(3)	−0.269 0(3)	0.725 41(14)	C(32R)	0.056 2(6)	0.218 3(5)	0.792 02(15)
C(5′)	0.786 0(11)	−0.401 7(9)	0.775 8(6)	C(33R)	0.037 7(6)	0.245 2(5)	0.739 99(15)
C(6′)	0.819 7(11)	−0.378 9(10)	0.824 0(5)	C(34R)	0.068 4(6)	0.340 3(5)	0.710 15(15)
S(7′)	0.680 2(3)	−0.275 8(3)	0.851 83(13)	C(35R)	0.117 6(6)	0.408 4(5)	0.732 34(15)
C(8′)	0.751 5(14)	−0.310 0(14)	0.913 7(3)	C(36R)	0.136 2(6)	0.381 5(5)	0.784 34(15)
C(9′)	0.660 3(18)	−0.226 0(6)	0.946 5(6)	C(37R)	0.220 4(6)	0.313 1(6)	0.894 84(24)
S(10′)	0.633 9(4)	−0.061 8(4)	0.926 61(15)	C(38R)	0.176 5(6)	0.441 7(6)	0.890 13(24)
S(13′)	0.873 6(4)	−0.009 9(4)	0.855 97(16)	C(39R)	0.255 2(6)	0.496 9(6)	0.901 95(24)
C(15′)	1.021 8(10)	−0.084 8(11)	0.774 3(4)	C(40R)	0.378 0(6)	0.423 4(6)	0.918 51(24)
B(1)	0.325 6(9)	0.751 8(9)	0.619 4(4)	C(41R)	0.421 9(6)	0.294 8(6)	0.923 23(24)
C(1R)	0.341 8(6)	0.717 8(5)	0.682 88(15)	C(42R)	0.343 1(6)	0.239 7(6)	0.911 39(24)
C(2R)	0.389 2(6)	0.786 6(5)	0.705 59(15)	C(43R)	−0.018 9(5)	0.308 1(5)	0.907 24(21)
C(3R)	0.404 4(6)	0.760 8(5)	0.757 80(15)	C(44R)	−0.024 8(5)	0.342 6(5)	0.954 09(21)
C(4R)	0.372 4(6)	0.666 2(5)	0.787 29(15)	C(45R)	−0.139 9(5)	0.381 1(5)	0.980 46(21)
C(5R)	0.325 1(6)	0.597 5(5)	0.764 61(15)	C(46R)	−0.249 2(5)	0.385 3(5)	0.959 95(21)
C(6R)	0.309 8(6)	0.623 3(5)	0.712 37(15)	C(47R)	−0.243 3(5)	0.350 8(5)	0.913 07(21)
C(7R)	0.264 5(6)	0.907 6(4)	0.602 35(22)	C(48R)	−0.128 2(5)	0.312 3(5)	0.886 71(21)
C(8R)	0.167 3(6)	0.977 9(4)	0.631 73(22)	C(12)	0.556 1(5)	0.027 1(5)	0.619 5(4)
C(9R)	0.113 9(6)	1.106 6(4)	0.617 74(22)	C(11′)	0.776 7(12)	−0.057 3(23)	0.949 95(17)
C(10R)	0.157 6(6)	1.165 1(4)	0.574 38(22)	C(12′)	0.887 2(5)	−0.115 0(17)	0.916 6(5)
C(11R)	0.254 7(6)	1.094 9(4)	0.545 01(22)	C(14′)	1.020 7(13)	−0.122 0(13)	0.830 7(4)
C(12R)	0.308 2(6)	0.966 2(4)	0.558 99(22)	C(11D)	0.738 7(18)	0.006 4(24)	0.944 3(5)
C(13R)	0.230 6(5)	0.689 4(5)	0.600 66(22)	C(12D)	0.870 0(11)	−0.058(3)	0.924 61(21)

Table 7 Bond lengths (Å), angles and torsion angles (°) with e.s.d.s for $[Ag([15]aneS_5)][B(C_6F_5)_4]$

Ag–S(1)	2.4712(19)	S(4)–C(5)	1.819(8)
Ag–S(4)	2.7262(20)	C(5)–C(6)	1.515(12)
Ag–S(7)	2.6847(21)	C(6)–S(7)	1.814(9)
Ag–S(10)	2.5621(19)	S(10)–C(11)	1.813(9)
Ag · · · S(13)	2.8813(19)	C(11)–C(12)	1.511(12)
S(1)–C(2)	1.815(7)	C(12)–S(13)	1.826(8)
S(1)–C(15)	1.819(8)	S(13)–C(14)	1.818(8)
C(2)–C(3)	1.531(10)	C(14)–C(15)	1.541(11)
C(3)–S(4)	1.804(8)		
S(1)–Ag–S(4)	85.20(6)	Ag–S(7)–C(8)	99.8(4)
S(1)–Ag–S(7)	127.86(6)	Ag–S(7)–C(8′)	87.0(5)
S(1)–Ag–S(10)	139.36(6)	C(6)–S(7)–C(8)	110.7(5)
S(1)–Ag–S(13)	82.64(6)	C(6)–S(7)–C(8′)	87.3(6)
S(4)–Ag–S(7)	80.64(6)	S(7)–C(8)–C(9)	113.6(8)
S(4)–Ag–S(10)	131.96(6)	C(8)–C(9)–S(10)	112.2(8)
S(4)–Ag–S(13)	90.29(6)	Ag–S(10)–C(9)	91.6(4)
S(7)–Ag–S(10)	81.01(6)	Ag–S(10)–C(11′)	101.3(3)
S(7)–Ag–S(13)	146.66(6)	Ag–S(10)–C(9′)	100.7(6)
S(10)–Ag–S(13)	81.59(6)	C(9)–S(10)–C(11)	96.1(5)
Ag–S(1)–C(2)	101.29(24)	C(11)–S(10)–C(9′)	109.8(6)
Ag–S(1)–C(15)	103.7(3)	S(10)–C(11)–C(12)	113.0(6)
C(2)–S(1)–C(15)	104.7(3)	C(11)–C(12)–S(13)	112.2(6)
S(1)–C(2)–C(3)	117.8(5)	Ag–S(13)–C(12)	94.0(3)
C(2)–C(3)–S(4)	118.3(5)	Ag–S(13)–C(14)	88.75(25)
Ag–S(4)–C(3)	98.56(24)	C(12)–S(13)–C(14)	102.2(4)
Ag–S(4)–C(5)	95.9(2)	S(13)–C(14)–C(15)	110.1(5)

Table 7 (*continued*)

C(3)–S(4)–C(5)	103.2(4)	S(1)–C(15)–C(14)	111.3(5)
S(4)–C(5)–C(6)	109.8(6)	S(7)–C(8′)–C(9′)	111.0(12)
C(5)–C(6)–S(7)	112.9(6)	S(10)–C(9′)–C(8′)	115.5(12)
Ag–S(7)–C(6)	100.6(3)		
C(15)–S(1)–C(2)–C(3)	−62.5(6)	S(7)–C(8)–C(9)–S(10)	−62.2(10)
C(2)–S(1)–C(15)–C(14)	146.5(5)	C(8)–C(9)–S(10)–C(11)	171.5(8)
S(1)–C(2)–C(3)–S(4)	−51.9(7)	C(9)–S(10)–C(11)–C(12)	−144.6(7)
C(2)–C(3)–S(4)–C(5)	−72.5(6)	C(9′)–S(10)–C(11)–C(12)	−157.6(8)
C(3)–S(4)–C(5)–C(6)	159.7(5)	C(11)–S(10)–C(9′)–C(8′)	96.7(13)
S(4)–C(5)–C(6)–S(7)	−74.8(6)	S(10)–C(11)–C(12)–S(13)	75.5(7)
C(5)–C(6)–S(7)–C(8)	146.1(6)	C(11)–C(12)–S(13)–C(14)	−138.3(6)
C(5)–C(6)–S(7)–C(8′)	127.8(8)	C(12)–S(13)–C(14)–C(15)	154.6(5)
C(6)–S(7)–C(8)–C(9)	−89.4(9)	S(13)–C(14)–C(15)–S(1)	−78.1(6)
C(6)–S(7)–C(8′)–C(9′)	−170.3(12)	S(7)–C(8′)–C(9′)–S(10)	60.1(15)

Table 8 Atomic coordinates with e.s.d.s for $[Ag([15]aneS_5)][B(C_6F_5)_4]$

Atom	*x*	*y*	*z*	Atom	*x*	*y*	*z*
Ag	1.001 91(4)	0.155 22(5)	1.044 51(4)	F(12)	0.339 7(3)	0.095 8(3)	0.748 13(24)
S(1)	0.950 89(14)	0.103 24(13)	1.168 15(12)	C(13R)	0.501 2(3)	0.330 6(3)	0.644 9(3)
C(2)	1.075 4(5)	0.197 5(5)	1.281 4(4)	C(14R)	0.621 3(3)	0.341 5(3)	0.690 0(3)
C(3)	1.114 7(6)	0.316 5(5)	1.295 7(5)	C(15R)	0.700 1(3)	0.370 5(3)	0.649 1(3)
S(4)	1.144 22(15)	0.346 44(14)	1.199 15(13)	C(16R)	0.658 9(3)	0.388 5(3)	0.563 1(3)
C(5)	1.283 8(5)	0.318 5(6)	1.209 4(5)	C(17R)	0.538 9(3)	0.377 6(3)	0.517 9(3)
C(6)	1.299 3(6)	0.300 1(6)	1.113 8(6)	C(18R)	0.460 0(3)	0.348 7(3)	0.558 8(3)
S(7)	1.204 90(15)	0.168 76(16)	1.016 80(13)	F(14)	0.665 8(3)	0.323 1(3)	0.769 22(25)
S(10)	0.917 05(14)	0.102 44(14)	0.858 02(12)	F(15)	0.813 9(3)	0.377 3(3)	0.689 9(3)
C(11)	0.812 8(7)	0.178 8(7)	0.844 3(5)	F(16)	0.735 5(4)	0.416 9(3)	0.523 4(3)
C(12)	0.727 8(6)	0.160 5(6)	0.892 6(5)	F(17)	0.500 0(4)	0.394 7(3)	0.435 2(3)
S(13)	0.798 83(14)	0.232 01(14)	1.026 47(12)	F(18)	0.349 2(3)	0.336 4(3)	0.511 52(25)
C(14)	0.739 4(5)	0.131 8(6)	1.067 3(5)	C(19R)	0.677 3(3)	−0.159 47(24)	0.410 61(23)
C(15)	0.825 7(6)	0.152 5(6)	1.171 5(5)	C(20R)	0.613 2(3)	−0.085 69(24)	0.416 14(23)
B	0.395 3(6)	0.285 2(6)	0.682 3(5)	C(21R)	0.663 6(3)	0.017 09(24)	0.492 92(23)
C(1R)	0.309 2(3)	0.368 4(3)	0.697 2(3)	C(22R)	0.778 2(3)	0.046 09(24)	0.564 18(23)
C(2R)	0.335 6(3)	0.472 9(3)	0.698 8(3)	C(23R)	0.842 3(3)	−0.027 69(24)	0.558 66(23)
C(3R)	0.262 8(3)	0.536 2(3)	0.716 8(3)	C(24R)	0.791 9(3)	−0.130 47(24)	0.481 87(23)
C(4R)	0.163 7(3)	0.495 0(3)	0.733 2(3)	F(20)	0.506 3(3)	−0.107 4(3)	0.351 02(25)
C(5R)	0.137 4(3)	0.390 5(3)	0.731 6(3)	F(21)	0.604 6(3)	0.090 2(3)	0.498 7(3)
C(6R)	0.210 1(3)	0.327 2(3)	0.713 6(3)	F(22)	0.829 2(4)	0.148 3(3)	0.635 6(3)
F(2)	0.430 4(3)	0.519 9(3)	0.690 3(3)	F(23)	0.952 2(3)	0.001 4(3)	0.626 3(3)
F(3)	0.286 6(3)	0.635 8(3)	0.717 4(3)	F(24)	0.856 9(3)	−0.195 8(3)	0.484 45(25)
F(4)	0.091 4(3)	0.556 3(3)	0.748 3(3)	C(1S)	1.511 8(7)	0.141 3(9)	0.301 8(6)
F(5)	0.042 2(3)	0.352 7(3)	0.747 6(3)	Cl(1S)	1.381 40(17)	0.111 00(17)	0.321 03(15)
F(6)	0.180 6(3)	0.229 7(3)	0.713 42(24)	Cl(2S)	1.489 75(22)	0.121 31(22)	0.182 48(17)
C(7R)	0.448 4(3)	0.281 6(3)	0.795 83(19)	C(2S)	0.911 6(7)	0.259 6(6)	1.500 6(5)
C(8R)	0.523 2(3)	0.380 1(3)	0.873 22(19)	Cl(3S)	0.975 96(20)	0.365 43(18)	1.474 79(16)
C(9R)	0.562 5(3)	0.387 7(3)	0.970 00(19)	Cl(4S)	0.826 51(20)	0.141 49(22)	1.395 94(15)
C(10R)	0.527 1(3)	0.296 8(3)	0.989 37(19)	Cl(5S)	−0.123 19(22)	0.487 35(19)	−0.013 20(20)
C(11R)	0.452 3(3)	0.198 4(3)	0.911 98(19)	C(8)	1.157 3(8)	0.177 6(10)	0.897 3(6)
C(12R)	0.412 9(3)	0.190 8(3)	0.815 20(19)	C(9)	1.042 7(7)	0.205 6(9)	0.869 1(9)
F(8)	0.557 3(3)	0.468 2(3)	0.859 62(25)	C(8′)	1.153 2(14)	0.241 9(13)	0.938 5(11)
F(9)	0.634 2(3)	0.481 9(3)	1.043 99(25)	C(9′)	1.047 8(11)	0.166 2(16)	0.843 5(11)
F(10)	0.565 2(3)	0.304 4(3)	1.083 08(25)	Ag′	1.002 8(10)	0.261 1(10)	1.070 1(8)
F(11)	0.420 7(3)	0.111 5(3)	0.931 1(3)	C(3S)	0.009 2(14)	0.499 6(14)	0.064 1(11)

occupancy 5.4% arising from a very small fragment of another crystal attached to the main crystal. As Ag is significantly heavier than any other atoms in the cation, no partial S or C atoms associated with this twin were identified. Hydrogen atoms were included in fixed, calculated positions and the phenyl rings of the $[B(C_6F_5)_4]^-$ counter ions were refined as rigid hexagons.

Selected bond lengths, angles and torsion angles are given in Table 7, fractional atomic coordinates in Table 8. Atomic scattering factors were inlaid,[24] or taken from ref. 28. Molecular geometry calculations utilised CALC[25] and the Figures were produced by ORTEP II.[29]

Additional material available from the Cambridge Crystallographic Data Centre comprises H-atom co-ordinates, thermal parameters and remaining bond lengths and angles.

Acknowledgements

We thank the SERC for support, the Royal Society of Edinburgh and Scottish Office Education Department for a Support Research Fellowship (to M. S.) and the Royal Society of London for a Fellowship (to D. C.).

References

1 M. Schröder, *Pure Appl. Chem.*, 1988, **60**, 517; A. J. Blake and M. Schröder, *Adv. Inorg. Chem.*, 1990, **35**, 1; G. Reid and M. Schröder, *Chem. Soc. Rev.*, 1990, **19**, 239.

2 S. R. Cooper, *Acc. Chem. Res.*, 1988, **21**, 141; S. C. Rawle and S. R. Cooper, *Struct. Bonding (Berlin)*, 1990, **72**, 1.

3 S. G. Murray and F. R. Hartley, *Chem. Rev.*, 1981, **81**, 365.

4 K. Wieghardt, H.-J. Kuppers and J. Weiss, *Inorg. Chem.*, 1985, **24**, 3067; A. J. Blake, A. J. Holder, T. I. Hyde and M. Schröder, *J. Chem. Soc., Chem. Commun.*, 1989, 1433.
5 A. J. Blake, R. O. Gould, M. A. Halcrow, A. J. Holder and M. Schröder, *J. Chem. Soc., Dalton Trans.*, 1992, 3427.
6 A. J. Blake, A. J. Holder, T. I. Hyde and M. Schröder, *J. Chem. Soc., Chem. Commun.*, 1987, 987.
7 A. J. Blake, R. O. Gould, A. J. Holder, T. I. Hyde and M. Schröder, *J. Chem. Soc., Dalton Trans.*, 1988, 1861; S. C. Rawle, R. Yagbasan, K. Prout and S. R. Cooper, *J. Am. Chem. Soc.*, 1987, **109**, 6181; S. R. Cooper, S. C. Rawle and R. Yagbasan, *J. Am. Chem. Soc.*, 1991, **113**, 1600; A. J. Blake, M. A. Halcrow and M. Schröder, *J. Chem. Soc., Chem. Commun.*, 1991, 253; D. Collison, G. Reid and M. Schröder, *Polyhedron*, in the press.
8 A. J. Blake, R. O. Gould, A. J. Holder, T. I. Hyde, G. Reid and M. Schröder, *J. Chem. Soc., Dalton Trans.*, 1990, 1759.
9 A. J. Blake, A. J. Holder, T. I. Hyde, Y. V. Roberts, A. J. Lavery and M. Schröder, *J. Organomet. Chem.*, 1987, **323**, 261; A. J. Blake, R. O. Gould, A. J. Lavery and M. Schröder, *Angew. Chem.*, 1986, **98**, 282; *Angew. Chem., Int. Ed. Engl.*, 1986, **25**, 274; G. Reid, A. J. Blake, T. I. Hyde and M. Schröder, *J. Chem. Soc., Chem. Commun.*, 1988, 1397; A. J. Blake, G. Reid and M. Schröder, *J. Chem. Soc., Dalton Trans.*, 1990, 3363.
10 A. J. Blake, R. O. Gould, A. J. Holder, T. I. Hyde, M. O. Odulate, A. J. Lavery and M. Schröder, *J. Chem. Soc., Chem. Commun.*, 1987, 118.
11 A. J. Blake, G. Reid and M. Schröder, *J. Chem. Soc., Dalton Trans.*, 1991, 615.
12 A. J. Blake, R. O. Gould, A. J. Holder, T. I. Hyde and M. Schröder, *Polyhedron*, 1989, **8**, 513.
13 A. J. Blake, R. O. Gould, J. A. Greig, A. J. Holder, T. I. Hyde and M. Schröder, *J. Chem. Soc., Chem. Commun.*, 1989, 876; A. J. Blake, J. A. Greig, A. J. Holder, T. I. Hyde, A. Taylor and M. Schröder, *Angew. Chem.*, 1990, **102**, 203; *Angew. Chem., Int. Ed. Engl.*, 1990, **29**, 197.
14 A. J. Blake, R. O. Gould, A. J. Holder, T. I. Hyde, G. Reid, A. Taylor, M. Schröder and D. Collison, *NATO ASI Series*, NATO Advanced Workshop on Molecular Electrochemistry of Inorganic, Bio-inorganic and Organometallic Compounds, eds. A. J. L. Pombeiro and J. A. McCleverty, Kluwer Academic Press, 1992, in the press.
15 J. Clarkson, R. Yagbasan, P. J. Blower, S. C. Rawle and S. R. Cooper, *J. Chem. Soc., Chem. Commun.*, 1987, 950; J. A. Clarkson, R. Yagbasan, P. J. Blower, S. C. Rawle and S. R. Cooper, *J. Chem. Soc., Chem. Commun.*, 1989, 1244; P. J. Blower, J. A. Clarkson, S. C. Rawle, J. R. Hartman, R. E. Wolf, R. Yagbasan, S. G. Bott and S. R. Cooper, *Inorg. Chem.*, 1989, **28**, 4040.
16 H.-J. Kuppers, K. Wieghardt, Y.-H. Tsay, C. Kruger, B. Nuber and J. Weiss, *Angew. Chem., Int. Ed. Engl.*, 1987, **26**, 575.
17 C. R. Lucas, S. Liu, M. J. Newlands, J.-P. Charland and E. J. Gabe, *Can. J. Chem.*, 1990, **68**, 644; J. Buter, R. M. Kellog and F. van Bolhuis, *J. Chem. Soc., Chem. Commun.*, 1991, 910; B. de Groot and S. J. Loeb, *Inorg. Chem.*, 1991, **30**, 3103; B. de Groot, G. R. Giesbiecht, S. J. Loeb and G. K. H. Shimizu, *Inorg. Chem.*, 1991, **30**, 177.
18 A. J. Blake, R. O. Gould, G. Reid and M. Schröder, *J. Chem. Soc., Chem. Commun.*, 1990, 974.
19 A. J. Blake, G. Reid and M. Schröder, *J. Chem. Soc., Chem. Commun.*, 1992, 1074.
20 J. Cragel, jun., V. B. Pett, M. D. Glick and R. E. DeSimone, *Inorg. Chem.*, 1978, **17**, 2885.
21 A. J. Blake, R. O. Gould, A. J. Lavery and M. Schröder, *Angew. Chem.*, 1986, **98**, 282; *Angew. Chem., Int. Ed. Engl.*, 1986, **25**, 274.
22 D. Collison and F. E. Mabbs, *J. Chem. Soc., Dalton Trans.*, 1982, 1565; B. Gahan and F. E. Mabbs, *J. Chem. Soc., Dalton Trans.*, 1983, 1713.
23 W. Clegg, *Acta Crystallogr., Sect. A*, 1981, **37**, 22.
24 SHELX 76, program for crystal structure refinement, G. M. Sheldrick, University of Cambridge, 1976.
25 CALC, program for molecular geometry calculations, R. O. Gould and P. Taylor, University of Edinburgh, 1985.
26 DIFABS, program for empirical absorption corrections, N. Walker and D. Stuart, *Acta Crystallogr., Sect. A*, 1983, **39**, 158.
27 J. Cosler and A. H. Glazer, *J. Appl. Crystallogr.*, 1986, **19**, 105.
28 D. T. Cromer and J. B. Mann, *Acta Crystallogr., Sect. A*, 1968, **24**, 321.
29 ORTEP II, interactive version, P. D. Mallinson and K. W. Muir, *J. Appl. Crystallogr.*, 1985, **18**, 51.

Received 6th August 1992; *Paper* 2/04252E